





## Article

# Hydrochemistry, Elements Distribution and Their Potential Recoveries in Gold Metallurgical Treatment Tailings Dams

Mariana Gazire Lemos <sup>1,2,\*</sup> , Teresa Maria Valente <sup>1</sup> , Amélia Paula Marinho Reis <sup>1</sup> , Amália Sequeira Braga <sup>1</sup>, Rita Maria Ferreira Fonseca <sup>3</sup> , Fernanda Guabiroba <sup>2</sup>, José Gregorio da Mata Filho <sup>2</sup>, Marcus Felix Magalhães <sup>2</sup>, Antonio Roberto Silva <sup>2</sup>, Apolo Pedrosa Bhering <sup>1</sup> and Giovana Rebelo Diório <sup>4</sup>

<sup>1</sup> Institute of Earth Sciences, University of Minho, Pole of University of Minho, Campus de Gualtar, 4710-057 Braga, Portugal; teresav@dct.uminho.pt (T.M.V.); pmarinho@dct.uminho.pt (A.P.M.R.); masbraga@dct.uminho.pt (A.S.B.); apolopb@yahoo.com.br (A.P.B.)

<sup>2</sup> AngloGold Ashanti, Mining and Technical, COO International, Nova Lima 34000-000, Brazil; fmguaabiroba@anglogoldashanti.com (F.G.); jgfilho@anglogoldashanti.com.br (J.G.d.M.F.); mfmagalhaes@anglogoldashanti.com.br (M.F.M.); bebetto@gmail.com (A.R.S.)

<sup>3</sup> Institute of Earth Sciences, University of Évora, Pole of University of Évora, 7000-345 Évora, Portugal; rfonseca@uevora.pt

<sup>4</sup> Laboratory on Basin Analysis, Universidade Federal do Paraná, Curitiba 81532-980, Brazil; g.rebelo.d@gmail.com

\* Correspondence: id8548@alunos.uminho.pt

**Abstract:** Wastewaters are valuable sources of metals and metalloids and can serve as essential resources for their recovery. Characterizing and understanding the occurrence of metals and other compounds, along with identifying the most effective recovery methods, are key steps in unlocking the potential for reusing these resources. The present study focused on analyzing waters from various mining dams in the Iron Quadrangle (IQ) region of Brazil, which contained metals such as Au, Cu, Ni, Zn, and sulfates resulting from the metallurgical treatment of Au. The results revealed a range of metal concentrations in the neutral zone in three tailings. Additionally, a 3D map was created, and a statistical analysis and an exploration of the processes governing mobility and partitioning were conducted to assess the potential for reuse. Notably, the study identified a high potential for Au recovery, particularly through the utilization of sustainable and cost-effective methods such as nanofibers with biosorbents. Overall, this research contributes to the understanding and exploration of potential reuse procedures for strategic metals in various industrial applications.

**Keywords:** circular economy; wastewater; mining tailings; Au recovery; hydrochemistry



**Citation:** Lemos, M.G.; Valente, T.M.; Reis, A.P.M.; Braga, A.S.; Fonseca, R.M.F.; Guabiroba, F.; Filho, J.G.d.M.; Magalhães, M.F.; Silva, A.R.; Bhering, A.P.; et al. Hydrochemistry, Elements Distribution and Their Potential Recoveries in Gold Metallurgical Treatment Tailings Dams. *Water* **2023**, *15*, 2714. <https://doi.org/10.3390/w15152714>

Academic Editor: Chi-Wang Li

Received: 28 June 2023

Revised: 19 July 2023

Accepted: 25 July 2023

Published: 27 July 2023



**Copyright:** © 2023 by the authors. Licensee MDPI, Basel, Switzerland. This article is an open access article distributed under the terms and conditions of the Creative Commons Attribution (CC BY) license (<https://creativecommons.org/licenses/by/4.0/>).

## 1. Introduction

Water is a critical issue throughout the entire mining cycle and within mining operations. The proper management of mine tailings has become a global and urgent concern. While the solid component of tailing dams is commonly studied, with several works highlighting the presence of toxic elements and their impacts [1–3], current research is increasingly focusing on transforming ore-extraction waste into valuable by-products [4–8], aligning with the principles of the circular economy. However, it is often overlooked that surface wastewater and groundwater are also present in these structures, and that they can contain various hazardous and potentially harmful substances. Consequently, it is crucial to monitor and manage these waters to prevent any adverse environmental impacts.

The characteristics of tailings wastewater vary depending on the type of mined ore and the mining and metallurgical processes involved [9]. Typically, these wastewaters contain high levels of suspended solids, including colloidal materials, that can increase concentrations of elements in free form and in various complexes (e.g., sulfates, carbonates, and nitrates), many of which are potentially toxic elements (PTE) [1,3]. Additionally, contaminants present in colloidal phases (>20 µm) and/or in solution have a greater impact

due to their higher reactivity and mobility [10–12]. Consequently, the characterization of wastewater from mining tailings is a complex yet crucial issue.

Surface water and interstitial water associated with the solid part of tailings can contain multiple elements that may pose environment and human health risks, including gold (Au), silver (Ag), nickel (Ni), manganese (Mn), iron (Fe), and aluminum (Al), as well as potentially hazardous substances such as mercury (Hg) and arsenic (As). Therefore, treatment processes, including neutralization, are usually required to minimize environmental impact [13]. Achieving knowledge about the environmental impact, risk assessment, and potential reuse of all components of mining tailings necessitates a comprehensive characterization of both the solids and water fractions. This involves employing various techniques, such as atomic absorption spectrometry (AAS) for trace metal concentration analysis, along with parameters such as pH, electrical conductivity (EC), turbidity, and suspended solids, associated with X-ray diffraction (XRD) to determine the mineralogy of suspended solids [3,14–16].

Understanding the occurrence of elements and the associated physicochemical parameters within these water bodies is crucial for identifying volume and distribution patterns [17–20]. Geostatistical and mathematical interpolation techniques, including kriging, cokriging, and inverse distance weighted, are commonly employed for 3D modeling groundwater parameters [19,21–24]. Additionally, understanding the hydrochemistry of tailings wastewater and the partitioning of elements among colloidal fractions is vital for assessing its potential for reuse [3,25,26].

To address this issue, governments and international organizations have implemented several measures to reduce the impact of mining tailings wastewater, including increasing public awareness [27,28]. As mining operations continue to grow in size and complexity, the management of tailings wastewater becomes increasingly crucial. In this context, reusing this wastewater can be an efficient and cost-effective approach to mitigating the environmental impact of mining while ensuring a reliable water source [29,30].

In recent years, numerous case studies have been conducted worldwide to explore the potential for water reuse from mining tailings, especially as water demand rises and the environmental impacts of mining become more apparent. It is crucial to treat and reuse mining tailings wastewater safely and sustainably. Such wastewater can be reused for various purposes, including crop irrigation, livestock water supply, and human consumption [31,32]. In some instances, artificial wetlands and lakes can be created, providing habitats for diverse flora and fauna [33,34]. Moreover, these wastewaters can be utilized for industrial processes such as cooling or energy generation [35,36].

In the case of Au tailings, previous studies have indicated a limited potential for wastewater reuse due to its hazardous nature [9,37–39]. This wastewater typically exhibits high concentrations of metal(loid)s such as copper (Cu), zinc (Zn), lead (Pb), and As, and may also contain organic compounds. Treatment processes such as sedimentation, flocculation, oxidation, and ion exchange are commonly employed to reduce the concentrations of these contaminants. Advanced treatments, such as membrane filtration, can also be applied to minimize associated risks.

Studies [40,41] have demonstrated the potential for metal recovery, including Au, in the circular economy context. These studies explored three subgroups, targeting solubility, size, charge, and reduction potential differences. In the same context, [42,43] also employed various technologies, including membrane technologies, adsorption, Fenton-based processes, advanced oxidation processes (AOP), and hybrid systems such as electrically enhanced membrane bioreactors (eMBRs) and integrated eMBR-adsorption systems. Other studies are evaluating techniques such as the biological precipitation of sulfides and the use of an aqueous solution of sodium alginate for direct gelation with metal ions [12,44,45]. Although these technologies represent significant advancements, further research is needed to enhance their effectiveness and suitability for industrial applications.

Once treated, wastewater can be reused for various purposes, including agricultural irrigation, industrial cooling water, and drinking water. However, before implementing

reuse strategies, a thorough assessment of the potential environmental impacts must be conducted [9,37,38,46,47].

In the case of Au tailings, reuse poses particular challenges. Au is often present in fine particulate form, which makes it difficult to separate from other elements. Moreover, Au is highly reactive and can form insoluble complexes with other elements, further complicating its recovery. Understanding the partitioning of Au among colloidal fractions is essential for evaluating its potential for reuse [26,48].

In the context described above, this study aims to characterize and compare the physicochemical properties of water from three Au tailings dams in the Iron Quadrangle, Brazil. The findings will provide valuable insights into the distribution of critical elements, laying the foundation for assessing reuse potential and implementing effective management strategies to minimize environmental impacts.

## 2. Study Area

The three tailing structures investigated in this study are located in the Iron Quadrangle (QF—Figure 1), Brazil's primary mineral province. Specifically, two tailing dams are situated in the city of Nova Lima and the third is in Santa Barbara, Minas Gerais. These cities have a long history of Au exploitation, dating back to the early 19th century, and remain important regions for Au production in Brazil. The gold deposits in these areas are hosted within the Rio das Velhas metallogenic Greenstone Belt, recognized as Brazil's most significant Au district [49,50].

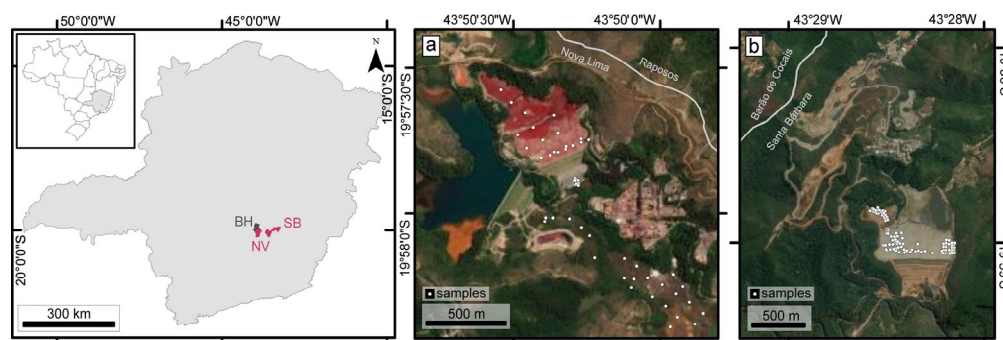


**Figure 1.** Location of the study areas in Minas Gerais State, near Belo Horizonte, Brazil, in red: (a) Nova Lima (NL) dams and deposits; and (b) Santa Barbara (SB) dams and deposits. The white markers indicate the locations of the samples.

A warm and temperate climate characterizes the QF region. The region experiences less rainfall during the winter when compared to summer. According to Köppen and Geiger's climate classification, the climate falls under the Cwa category. The average temperature in the region is 20.4 °C, with an annual rainfall of 1551 mm. Due to the temperate climate, categorizing the seasons can be challenging [8,51,52].

The Santa Barbara tailings dam is in the northern part of the QF, in Santa Barbara, Minas Gerais, ca. 110 km from Belo Horizonte. Since 1986, waste from underground Au metallurgical plants has been deposited in this structure. As the workflow reviewed by [8] identified, the waste for these structures has different origins: (a) waste from a flotation plant and (b) waste from the leaching stage, both derived from freshly underground mined ores [53,54]. According to [55], solid tailings from this dam contain minerals such as quartz, muscovite, and biotite, as well as phases formed during the processing stages, including gypsum, jarosite, and iron antimonate. Arsenic (As) is also associated with phases such as antimony oxide and is occasionally found in arsenopyrite. Chemically, elements such as Fe, Au, antimony (Sb), sulfur (S), As, and Cu are present. The surface waters of this dam were reported to be alkaline, with maximum pH values of ca. 10, and contained potentially toxic elements such as Sb, As, and Cu. The average water volume of this dam during the sampled period was 1766.25 m<sup>3</sup> [51].

The Nova Lima dams and tailings deposits are located in the northern part of the QF, ca. 25 km from the capital Belo Horizonte, Minas Gerais. These dams are part of the Queiroz metallurgical plant, which has been treating sulfide Au ores for over thirty years. The materials processed in the plant are divided into two distinct circuits, as summarized by [8]. The Raposos circuit treats non-refractory sulfide ore (pyrite, pyrrhotite, and subordinate arsenopyrite), mainly from the Raposos mines. The circuit involves grinding, gravity concentration, conventional leaching, carbon-in-leach (CIL), elution, and electrowinning, achieving 90% Au recovery. The tailings generated in this circuit were deposited in the Cocoruto tailings impoundment (CO). This part of the plant was deactivated in 1998 with the closure of the Raposos underground mine [48,51,56]. The Cocoruto dam (old circuit) mainly consists of quartz, carbonates, iron oxides, and phyllosilicates such as muscovite and chlorite [48]. Chemically, it contains Fe > calcium (Ca) > magnesium (Mg) > Al > Mn > potassium (K), and sodium (Na).

Currently, the Queiroz plant circuit processes refractory Au ore, which requires a calcination step after grinding and flotation. After calcination, Au is recovered through conventional leaching, CIL, elution, and electrowinning [48,51,56]. The generated tailings are deposited in the Calcination dam (CA). According to [8], this type of residue undergoes significant mineralogical transformations between the source and the storage location. All concentrated sulfides are subjected to high-temperature c and are thus calcined, which explains the enrichment of iron oxides in elements such as As, Cu, Ni, Ag, and Au. Gypsum is also observed, likely formed by adding reagents such as lime during the calcination process. The water volumes of these dams are 142,000 m<sup>3</sup> for Cocoruto and 23,792 m<sup>3</sup> for Calcinados [51].

### 3. Methodology

Figure 2 summarizes the workflow used in this study.

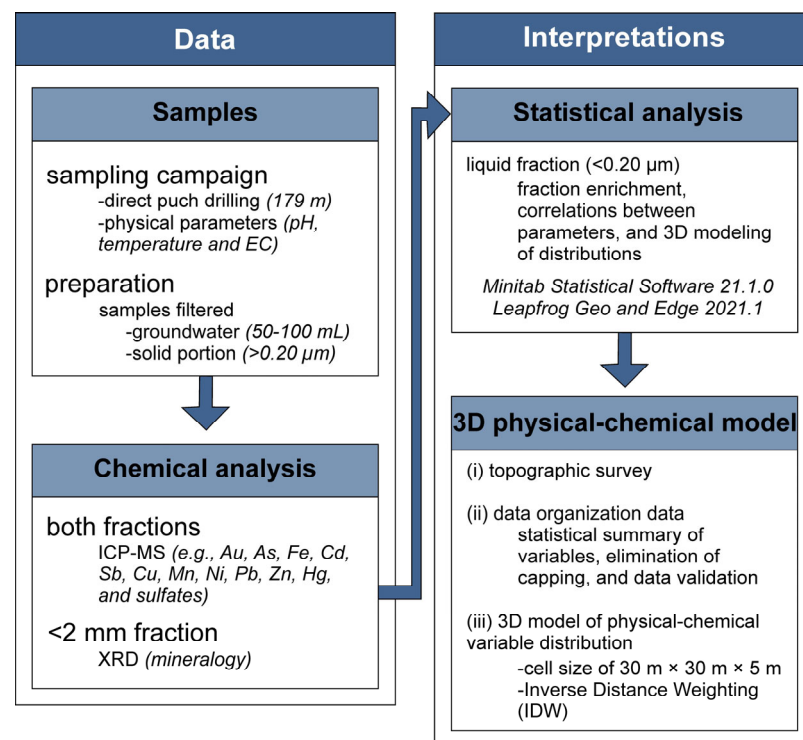


**Figure 2.** Workflow of the methodological approach.

The sampling campaign took place during winter and early spring (May–September 2020). During these months, the weather conditions are typically dry, with temperatures ranging from 15 to 25 °C [57].

The samples were collected using direct push drilling methods, with a maximum depth of 20 m, resulting in 179 m of samples (Figure 1 and Figure S1). Each sample represented a 1-m depth interval; during the probing process, a sample was collected for every 1-m advance. The samples were filtered using 0.20 µm syringe filters to separate the groundwater. Aliquots of the liquid phase (50–100 mL) were stored in polypropylene bottles, acidified to pH < 2, and kept in the dark at 5 °C for chemical analysis. The solid fraction (>0.20 µm) was placed in plastic bags and sent for chemical analysis. Evaluating both fractions is essential for understanding the mobility of elements in groundwater from these structures.

At each sampling site, parameters such as pH, temperature, and EC were measured using methods described in the Standard Methods of Water and Wastewater [52]. Weak Acid Dissociable Cyanide (CN<sub>Wad</sub>), which refers to a group of cyanide species defined operationally that release free cyanide when refluxed under weakly acidic conditions (pH 4.5–6), was also measured using the same standard methods [52]. Elements such as Au, As, Fe, cadmium (Cd), Sb, Cu, Mn, Ni, Pb, Zn, Hg, and sulfates were analyzed using inductively coupled plasma mass spectrometry (ICP-MS) for both fractions. Blanks, replicates, and stock solutions were used to ensure quality control.

To understand possible sources of chemical element distribution in wastewater samples, a mineralogical study was conducted using X-ray diffraction (XRD) with a X'pert Pro-MPD diffractometer (Philips PW 1710, APD) using CuKα radiation, equipped with an automatic divergence slit and a graphite monochromator. Diffractograms were obtained from powders of the <2 mm fraction, covering the 3 to 65 °2θ range, with a 2θ step size of 0.02° and a counting time of 1.25 s.

For interpretation, statistical analysis, such as correlations between parameters and determination of enrichment factors (E<sub>fx</sub>), were performed using Minitab Statistical Software version 21.1.0, as well as 3D modeling of parameters distributions in the liquid fraction (<0.20 µm) using Leapfrog Geo and Edge 2021.1.

The E<sub>fx</sub> can be calculated to express the ratio between the concentration of elements in the fraction smaller than 20 µm (aqueous phase—X<sub>fraction</sub>) compared to the fraction above 0.20 µm (X<sub>solids</sub>). This factor is particularly relevant for elements of higher environmental concern [46]. The E<sub>fx</sub> can be calculated using Equation (1) [58,59]:

$$E_{fx} = X_{fraction}/X_{solids} \quad (1)$$

The construction of the 3D physical-chemical model involved three steps: (i) conducting a topographic survey of the dam and sampled points using a total station; (ii) organizing the topographic and physical-chemical data, performing a statistical summary of variables, eliminating the capping, and validating the data; and (iii) estimating and constructing the 3D model of the distribution of physical-chemical variables, and validating the models.

All the models are 3D block models with a discretization cell size of 30 m × 30 m × 5 m [8, 19,60]. For step 3, the geostatistical interpolation method, called Inverse Distance Weighting (IDW), was employed. IDW is a commonly used technique in water resources management [19,61,62]. It estimated values based on known nearby locations, and the assigned weights to the interpolating points are inversely proportional to their distance from the interpolation point. In other words, closer points have higher weights when compared to distant points, and vice versa [19,22]. In this study, a fifth power weight was utilized to limit the influence of samples in distant regions and refine the estimation [59].

## 4. Results and Discussions

### 4.1. Groundwater Composition and Hydrochemical Relationships

The parameters measured in situ, along with others, serve as primary indicators of the characteristics of each structure and their distinguishing factors [63].

Tables 1 and 2 present statistical summaries of the elements and physicochemical parameters (pH and EC) for water samples from the three structures and their interrelationships. Overall, the water samples exhibit elevated concentrations of metals, and

despite having pH levels close to neutral, attention must be paid to potential sources of contamination, as certain elements exceed the maximum values according to Brazilian regulations for Class II freshwater [64].

**Table 1.** Statistical summary of chemical variables of wastewater from CO, CA, and CDS2 tailing deposits.

Structure	pH	EC	CN Wad	Au	Cd	Hg	Mn	Zn	Pb	Cu	Fe	Ni	SO <sub>4</sub> <sup>4-</sup>	As	Sb	Co	
		μS/cm	mg/L	mg/L													
Cocoruto (CO)	Mean	6.90	2585	0.025	0.0250	0.0005	0.001	1.72	0.0125	0.012	0.015	0.9	0.03	1270.8	0.006	0.001	0.0005
	Max	8.67	4036	0.078	0.0250	0.0005	0.001	24.61	0.1000	0.061	0.224	6.1	0.42	5444.5	0.026	0.001	0.0005
	Min	6.08	1390	0.025	0.0250	0.0005	0.001	0.03	0.0100	0.005	0.004	0.1	0.01	33.3	0.005	0.001	0.0005
	SD	0.5867	877	0.0024	0.0000	0.0000	0.000	3.54	0.0133	0.016	0.034	1.2	0.06	892.3	0.004	0.000	0.0000
Calcinado (CA)	Mean	9.07	4402	28.9	0.0280	0.0005	0.001	0.10	0.1018	0.005	1285	0.2	0.39	1989.1	0.005	0.001	0.0005
	Max	10.44	6947	88.0	0.0800	0.0005	0.001	0.62	1.1000	0.028	46523	2.2	9.12	2820.4	0.005	0.001	0.0005
	Min	2.92	2367	6.0	0.0250	0.0005	0.001	0.01	0.0100	0.005	0.0	0.1	0.01	1337.1	0.005	0.001	0.0005
	SD	1.187	1065	14.50	0.0129	0.0000	0.000	0.14	0.2328	0.003	5698.7	0.4	1.32	355.7	0.000	0.000	0.0000
CDS2	Mean	7.32	3808	11.240	0.0408	0.0100	0.001	0.02	0.0104	0.107	19.3	0.1	1.94	2234.7	1.6	4.0	0.0100
	Max	8.03	4460	7.920	0.3000	0.0100	0.001	0.02	0.0159	0.191	20.7	0.4	2.62	3500.0	25.6	23.8	0.0100
	Min	6.66	3455	13.700	0.0250	0.0100	0.001	0.02	0.0050	0.040	14.1	0.0	0.01	1608.0	0.0	0.5	0.0100
	SD	0.3592	229	1.000	0.0519	0.0000	0.000	0.00	0.0040	0.053	1.6	0.1	1.10	687.5	6.2	5.1	0.0000

Note: SD = standard deviation; Min—Minimum; Max—Maximum.

**Table 2.** Correlation between the collected parameters for the three dams using Pearson Coefficient. Medium to strongest correlations ( $r^2 > 0.25$ ) are highlighted in green.

	pH	EC	Au	Cd	Mn	Zn	Pb	Fe	Cu	Ni	SO <sub>4</sub> <sup>2-</sup>	As	Sb
		μS/cm	mg/L										
pH	1.00												
EC	0.568	1.00											
Au	0.008	0.077	1.00										
Cd	-0.114	0.198	0.319	1.00									
Mn	-0.160	-0.125	-0.041	-0.140	1.00								
Zn	0.315	0.214	-0.035	-0.130	-0.034	1.00							
Pb	-0.122	0.193	0.292	0.903	-0.030	-0.140	1.00						
Fe	-0.114	-0.232	-0.046	-0.191	0.385	-0.026	-0.086	1.00					
Cu	0.275	0.099	-0.020	-0.068	-0.042	-0.021	-0.075	-0.061	1.00				
Ni	0.137	0.160	0.172	0.417	-0.086	-0.063	0.377	-0.134	0.747	1.00			
SO <sub>4</sub> <sup>2-</sup>	0.376	0.401	0.066	0.131	0.336	0.042	0.088	-0.175	0.143	0.227	1.00		
As	-0.032	0.013	-0.007	0.263	-0.026	-0.022	0.047	-0.039	-0.013	0.133	0.055	1.00	
Sb	-0.066	0.093	0.334	0.761	-0.091	-0.080	0.389	-0.125	-0.044	0.271	0.154	0.256	1.00

In terms of physicochemical characteristics, it is observed that the waters from the Cocoruto and CDS2 dams exhibit similar pH levels, ranging from 6 to 8. However, the sampled waters from the Calcinados dam have a higher alkaline pH, with values above 8. The average EC ranges from 2585 μS/cm to 4402 μS/cm, indicating distinct and higher values for the Calcinados and CDS2 dams. In general, this variable (EC) may be directly linked to sulfate concentrations, which are relatively high for all structures (1270 to 5444 mg/L) and have a Pearson correlation coefficient of 0.4 (Table 2 and Figure S1a–c). Additionally, there is a clear relationship (above 0.5) between pH and EC, indicating zones of mineral-effluent interaction, mainly due to sulfides and sulfates.

The metal concentrations (loids) are essential indicators for differentiating waters and classifying these structures [3]. The Ficklin diagram (Figure 3), as described by [63], can express this differentiation. In the studied structures, Co and Cd showed values close to the detection limits of the method. At the same time, the concentrations of Zn, Pb, Ni, and Cu were considerable and varied depending on the evaluated dam.

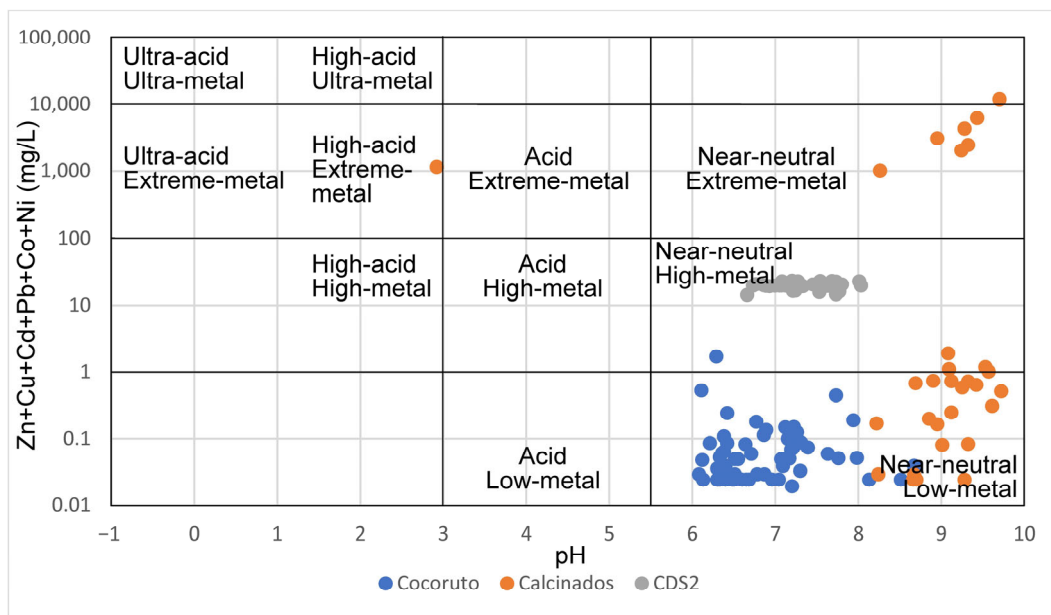


**Figure 3.** Projection of the samples for the three dams according to the Ficklin Diagram.

The sampled waters in Cocoruto are essentially classified as near-neutral low-metal. The waters from CDS2 belong to the near-neutral high-metal zones, while Calcinados exhibited distinct classifications. In Calcinados, 70% of the sampled points fall under near-neutral low-metal zones; the remaining 30% fall under near-neutral extreme-metal zones. One point in Calcinados was classified as high-acid high-metal and will be disregarded.

The differences observed in Figure 3 for Calcinados are directly related to the Cu content and are associated with the location within the specific dam. Points classified as high-metal may be influenced by the discharge of effluents from the plant during a period of low efficiency, changes in feed sources, or alterations in the beneficiation process, such as the inclusion of other reagents that may contain this metal [48]. The maps in Figure 4 highlight zones with higher metal contents, particularly Cu, Zn, Ni, and sulfates.

In Figure 4, it is observed that in the Calcinados dam, water zones with higher concentrations of Cu, Au, Ni, and sulfates are correlated at depths between 0–10 and 10–20 m. Figure S2 and Table 2 confirm this relationship. Additionally, some sulfate-rich zones also show a correlation with Fe. Controversially, Zn, Mn, and, in some parts, Fe indicate enrichment in other parts of the dam (Figures 4 and S2a), and their concentrations increase with depth in the interstitial waters (Figure S3a). The relationship between the concentration of these elements and depth may be due to variations in physical parameters such as pH and EC (Figure S3a).

In the Cocoruto dam, Au concentrations were below the detection limit, preventing the generation of a variability map. Cu shows higher concentrations in the NW portion, up to depths of ca. 15 m, which may be related to the influences of reagents used in the plant (Figure 4) [56]. Zn is also concentrated in this region but to a greater extent in the SE part. Furthermore, in Figure S2b, these elements exhibit a high Pearson coefficient (above 0.90). The other elements, although found in smaller zones of high concentration alongside Cu, have a greater extent in the opposite portion near the dam spillway and at lower elevations [51]. There is a clear relationship between Fe, Mn, and sulfates, also observed in the Pearson correlation matrix in Figure S2b and Table 2. Only Fe shows an enrichment relationship at greater depths (Figure S3b) regarding variation vs. depth. This influence may be attributed to the treatment of ores rich in this element, particularly in banded iron formations, which are abundant in Fe-carbonates such as siderite during the early years of operation of the older mines that supplied the metallurgical circuit [48,65]. Furthermore, a clear variation is observed with decreasing pH and increasing EC in deeper regions of this dam (Figure S3b).

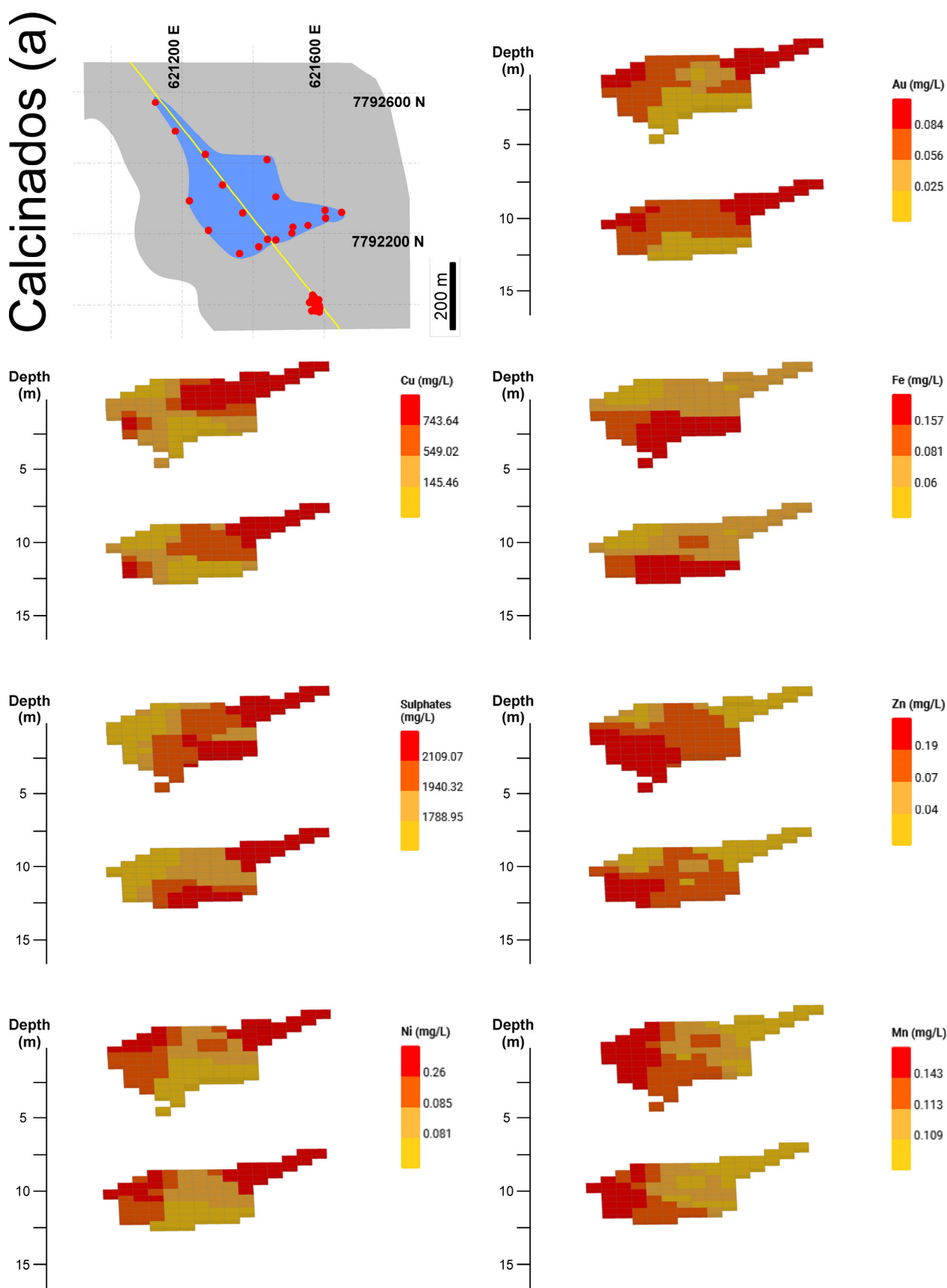


Figure 4. Cont.



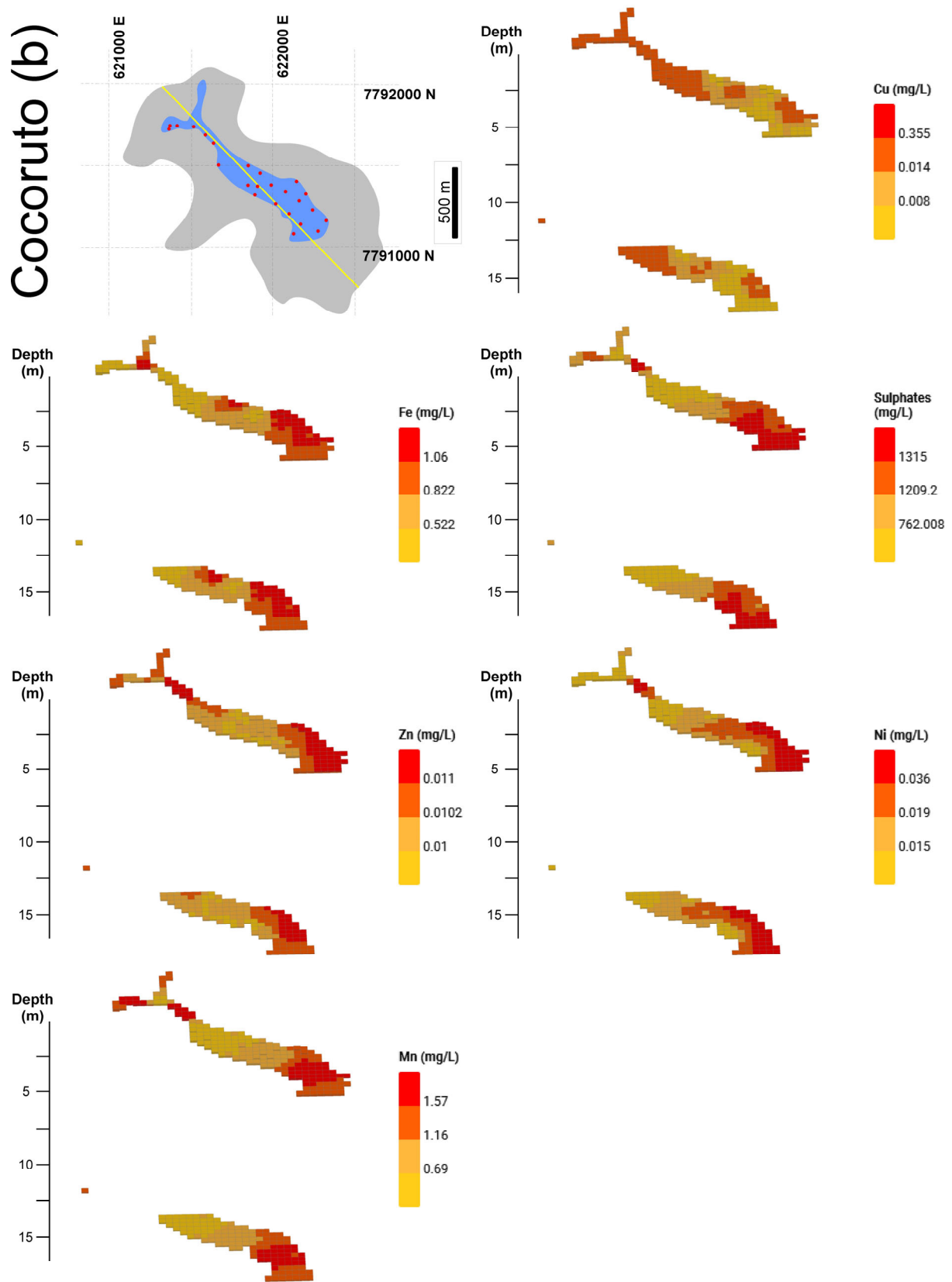
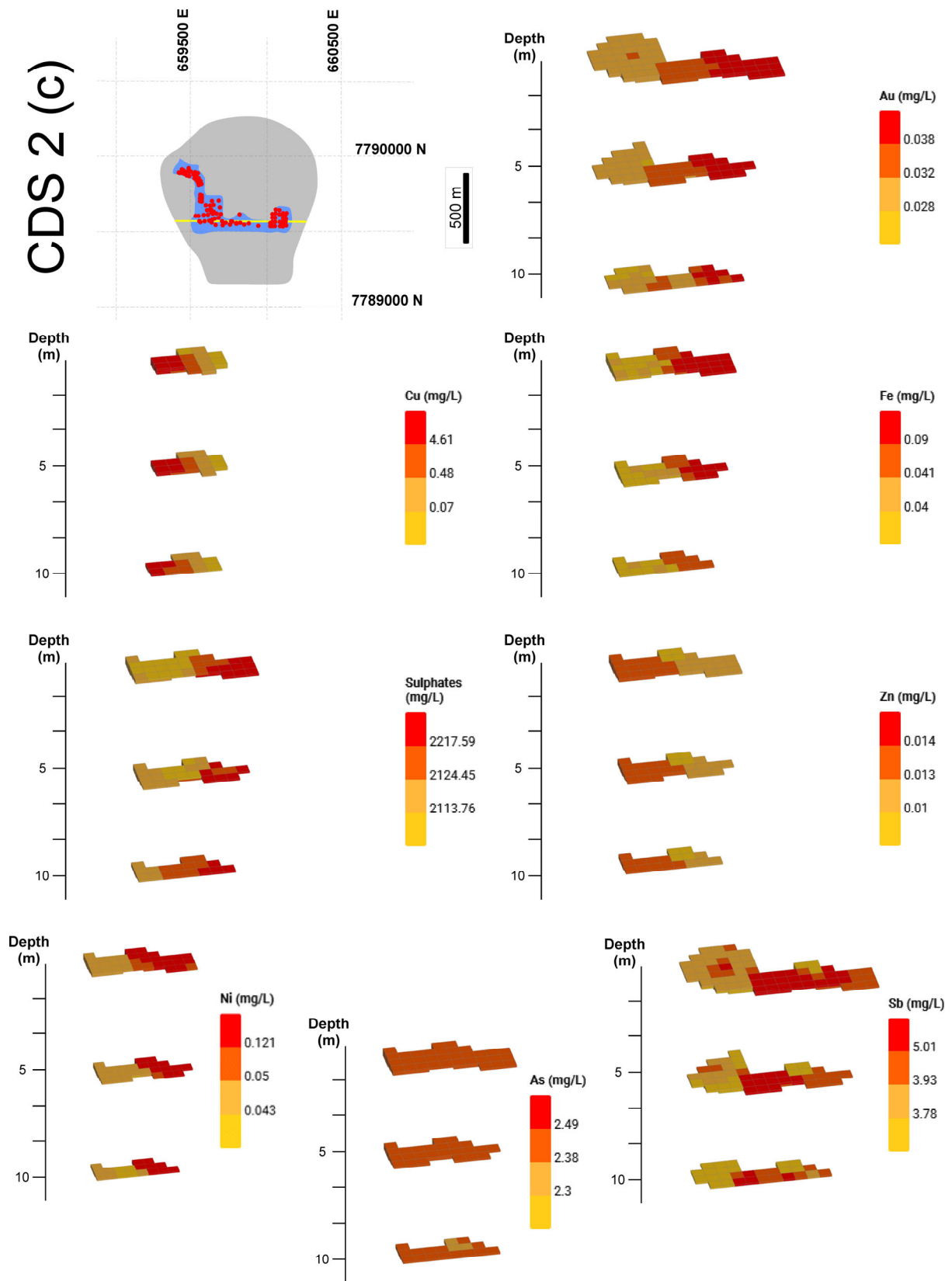


Figure 4. Cont.



**Figure 4.** 3D distribution of the concentrations of the main elements in the water of the three dams: (a) Calcinados, (b) Cocoruto, and (c) CDS2.

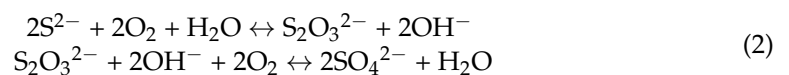
In the CDS2 dam, Mn concentrations remained below the detection limit. Among the highest concentrations within the sampled region, there is a concentration relationship among all elements except for Zn, which only shows an enrichment relationship with As by region and depth (Figures 4 and S2c). A positive correlation is observed between sulfates and elements such as As and Fe (Pearson coefficient of Figure S2c). The increase in Au concentration is accompanied by enrichments, mainly with Sb and As (Table 2 and Figure S2c). Differences in ore types and the types of reagents used in the processing plant may contribute to these concentration variations [55]. The discharge of the plant effluent, which is not fixed, may also result in spatial differences in the distribution pattern of some soluble elements [51]. Regarding the variation of elements with depth, the mid-depth portions (up to 8 m) generally exhibit higher enrichments than deeper regions (Figure S3c). This pattern is not observed for Zn and Fe, which also increase in concentration near 15 m. The availability of Fe sulfides and possibly Zn may be relatively high at depth, and the environment is more prone to the dissolution of these elements, even with high pH and low EC variation (Figure S3b). This can be supported by the fact that the processing plant in this region initially received feed from pyrite, ankerite, siderite, and magnetite-rich bodies, with subordinate sphalerite, arsenopyrite, and berthierite, which are the sources of the current mineralization [53,55].

#### 4.2. Mineral-Water Interaction and Enrichment Factors

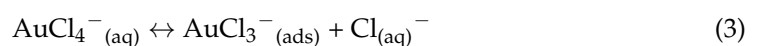
The analysis of mineral-water interaction utilizes a set of physicochemical parameters that are considered relevant due to their forms of occurrence, attributed toxicity, and their role in the geochemical evolution of the system under study [66]. Furthermore, understanding the interactions between solids and water is crucial for developing tools for extracting and potentially reusing soluble elements in these types of waters [55].

Figure 5 illustrates the average Efx between the water and the accumulated solids (<0.20 µm) in these dams. The characteristics of the solid waste are summarized in Tables S1 and S2 and described in detail by [8,48,55]. Generally, the Efx for the solid fraction is low, but the accumulation of elements such as Au and total S in the effluents should not be disregarded. Specifically, the samples representing Cocoruto show enrichment in Mn (Figure 5b), and the Calcinados samples and the CDS2 samples exhibit enrichment in Cu (Figure 5a,c). The CDS2 samples also demonstrate higher Pb, Sb, and Ni enrichment.

Considering the mineral-water interaction model developed by [66], the chemical composition of these effluents can be explained by two main factors: (i) the influence of mineral solubility and (ii) the influence of surface interaction. Based on factor (i) and the pH conditions measured in these dams, it can be inferred that the concentrations of S originated from sulfides and sulfates (Table S1 and Equation (2)). Reagents such as Cu-sulfate, which are used in Au processing, may also contribute to these interactions.



Other metals, including Au, are also enriched in the three dams, although the process of Au enrichment involves additional complexities that require complementary analyses beyond the scope of this study. If Au is present in an aqueous medium as Au (III) or Au (I) complexed with Cl in the form of AuCl<sub>4</sub><sup>−</sup> (Equation (3)), for instance, it is possible that the complexation is a result of the release of chloride ions from a source such as processing reagents [66]. Furthermore, the presence of Au in a soluble form may be attributed to beneficiation steps, as the effluents are discharged into the dam. This observation may be related to the presence of residual cyanide (CN), as indicated in Table 1, and the alkaline pH conditions (as shown in Equation (4)) [67]:



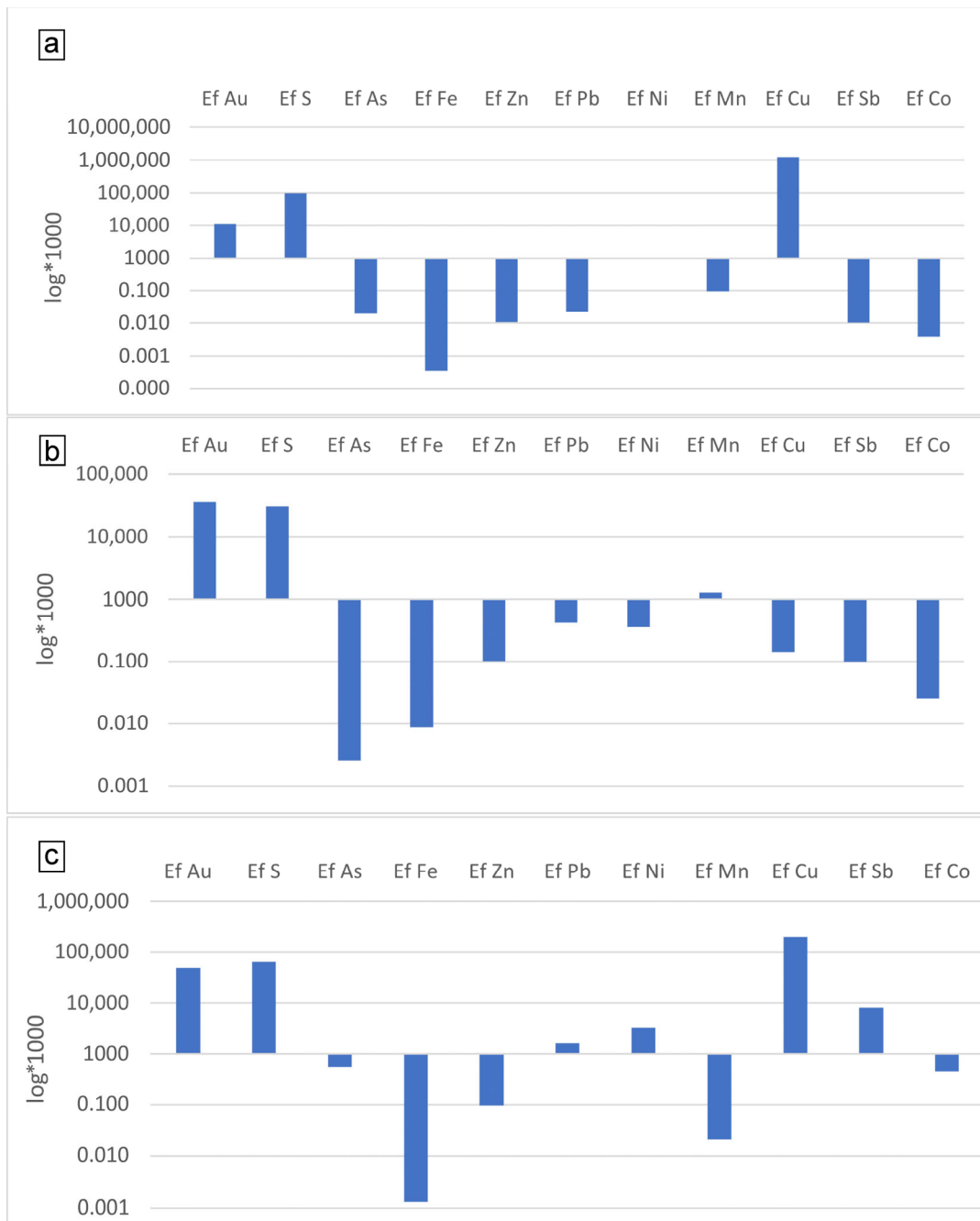
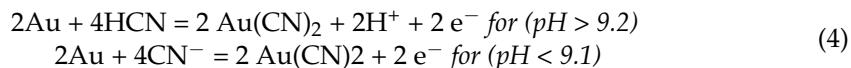


**Figure 5.** Enrichment ratio of the liquid to solid fraction (Ef) in each tailing dam: (a) Calcinados, (b) Cocoruto, and (c) CDS2.

The environmental conditions of the three dams can facilitate such reactions if the redox potential (eH) is above 1 V or in natural temperature and pressure conditions [53]. It is known that in some cases, the beneficiation of Au ores undergoes oxidation under pressure and temperature environments that promote the formation of Au complexes with Cl and CN, which remain stable in an aqueous medium under natural conditions [53]. However, further investigation is necessary to draw conclusive hypotheses regarding these

processes. In addition, there may be a significant contribution of nano-sized Au particles below 2  $\mu\text{m}$ , either released or adsorbed onto other nanometric compounds.

In the Cocoruto dam, the Efx of Mn in the effluent is also noteworthy, and its primary source is carbonates (Table S1). The availability of Mn ions can occur at a pH close to 8 when the eH ranges from  $-0.2$  to  $0.4$  v [68]. The contribution of Mn-containing nanoparticles cannot be ruled out.

Regarding Cu and Ni, mechanisms similar to those observed for Au can occur in these environments. The presence of residual CN in the dams or during the beneficiation process can lead to the formation of stable complexes in aqueous media, such as  $\text{Cu}(\text{CN})_3^{2-}$  and  $\text{Ni}(\text{CN})_4$  [53]. The oxidation of sulfides in the tailings can also result in the formation of complexes containing Cu and Ni in water, as sulfides containing these elements are present, especially in the CDS2 dam. These sulfides can react with cyanide or other lixiviating agents, such as Cl and F, leading to reactions and the stability of these complexes in the aqueous environment [53].

In the case of the CDS2 dam, the influence of Sb in the groundwater samples was also observed. Specifically, the solids in this dam originate from a sulfide called berthierite (Table S1). The presence of this sulfide in an environment with a high pH (above 9) and leachability, such as CN, contributed to its stability in the soluble form [53]. Therefore, the presence of Sb is likely due to this mechanism.

#### 4.3. Metal Concentrations in Tailing Waters and the Key to Reuse

Based on the discussed characteristics and understanding of possible mechanisms, a strategy for metal extraction and water reuse in industrial environments is proposed in this study.

The water contained in these three dams is present in active industrial settings. Therefore, besides the potential for extracting metal(loid)s in high concentrations, the water can also be reused within metallurgical plants or for non-industrial purposes, such as supplying administrative areas of the facility.

In this regard, sustainable alternatives for metal extraction, such as the use of biosorbents, are presented. Among various suggested techniques [40–42,44,45,69], using biosorbents, specifically nanofibers with chelating properties, was the most viable and sustainable method for this study. The work conducted by [43] used water samples from these dams, as described in previous sections, and aimed to recover Au (III), Cu (II), Ni (II), and other metals using nanofibers made from *Bixa orellana* Linnaeus (URU), a native Brazilian plant known for its chelating properties. The nanofibers were prepared by combining URU seed powder with a polycaprolactone polymer (PCL). The recovery tests were carried out using a pure solution at pH 2, room temperature ( $25\text{ }^\circ\text{C}$ ), and a contact time of 24 h [70].

The results from the water samples collected from these dams, as presented in Table 3 (adapted from [70]), demonstrate a significant potential for sustainable extraction, particularly for Au.

**Table 3.** Recovery results of Au and other metals using nanofiber containing URU—Adapted from [43,70].

Element	Mean	Min	Max	SD
		%		
Au (III)	75.898	84.35	58.726	6.043
Cu (II)	2.726	6.647	0.354	1.983
Ni (II)	2.099	4.614	0.045	1.419
Pb (II)	28.488	43.835	21.77	7.029
Zn (II)	4.274	7.09	2.294	1.447
Co (II)	4.299	7.889	1.083	2.252

The obtained results indicate that PCL nanofibers containing Urucum have the potential to be applied in the recovery of strategic metals for the sustainability of these

wastewaters. This approach opens numerous possibilities for use, such as effluents treatment and other technological initiatives that can be developed, driven by its low cost. Furthermore, this system offers the opportunity for metal extraction and the reuse of two types of valuable resources: metals and water.

## 5. Conclusions

Despite being located in the same region (QF), the characterized waters showed distinct properties, with varying projections ranging from neutral with high to low metal availability, as classified in the Ficklin Diagram. However, even in samples of low availability, the concentration of certain elements, including Au, Ni, Cu, and S (mainly in the form of sulfates), was not negligible. The characterization steps guided the selection of a technique that demonstrated potential for the recovery of metals, mainly Au.

The distribution of these elements across the three structures and the governing mechanisms of their mobility are crucial factors for their potential recovery. In a specific case study using water samples from the CDS2 dam, nanomembranes containing *Bixa orellana Linnaeus* seeds successfully recovered these elements, especially Au. This work serves as an example of sustainable recovery and purification of these waters at a low cost when compared to other options.

Therefore, this research contributes to the potential reuse of strategic metals in the industry. Furthermore, it demonstrates the possibility of obtaining water free of toxic elements or within permissible limits set by environmental regulations, enabling more sustainable management of water resources by using water from the mining tailings.

**Supplementary Materials:** The following supporting information can be downloaded at: <https://www.mdpi.com/article/10.3390/w15152714/s1>. Figure S1. (a) Location of sample points in plan and depth for each structure: (b) Calcinados, (c) Cocoruto, and (d) Santa Barbara. Figure S2. Correlogram matrix of physicochemical variables of groundwater by structure: (a) Calcinados, (b) Cocoruto, and (c) CDS2. Figure S3. Distribution of elements by depth in structure: (a) Calcinados, (b) Cocoruto, and (c) Santa Barbara. Table S1. Mineralogy of the solid fraction of the Calcinados, Cocoruto, and CDS2 tailings dams—Adapted from [8]. Table S2. Statistical summary of the chemistry of the solid fractions of the Calcinados, Cocoruto, and CDS2 tailings dams—Adapted from [8].

**Author Contributions:** M.G.L., T.M.V., A.P.M.R., R.M.F.F., F.G., J.G.d.M.F. and M.F.M.; methodology, M.G.L., T.M.V., A.P.M.R., A.R.S., R.M.F.F., F.G., J.G.d.M.F., A.S.B. and M.F.M.; software, M.G.L.; validation, M.G.L., T.M.V., A.P.M.R., R.M.F.F., F.G., J.G.d.M.F. and M.F.M.; formal analysis, M.G.L., T.M.V., A.P.M.R., R.M.F.F., F.G., J.G.d.M.F. and M.F.M.; investigation, M.G.L., T.M.V., A.P.M.R., R.M.F.F., F.G., J.G.d.M.F. and M.F.M.; resources, M.G.L., T.M.V., A.P.M.R., R.M.F.F., F.G., J.G.d.M.F. and M.F.M.; data curation, M.G.L., T.M.V., A.P.M.R. and R.M.F.F.; writing—original draft preparation, M.G.L. and A.P.B.; writing—review and editing, M.G.L., T.M.V., A.P.M.R., R.M.F.F. and G.R.D.; visualization, M.G.L., T.M.V., A.P.M.R., R.M.F.F. and G.R.D.; supervision, T.M.V., A.P.M.R. and R.M.F.F.; project administration, M.G.L., T.M.V., A.P.M.R., R.M.F.F., F.G., J.G.d.M.F. and M.F.M.; funding acquisition, M.G.L., T.M.V., A.P.M.R., R.M.F.F., F.G., J.G.d.M.F. and M.F.M. All authors have read and agreed to the published version of the manuscript.

**Funding:** This research was funded by Fundação para a Ciência and Tecnologia (FCT) through projects UIDB/04683/2020, UIDP/04683/2020, and Nano-MINENV 029259 (PTDC/CTA-AMB/29259/2017).

**Data Availability Statement:** The data presented in this study are available upon request from the corresponding author. The data are not publicly available due to high amounts of data.

**Acknowledgments:** We thank our colleagues from the Instituto de Ciências da Terra (ICT), the Microscopy Center from Universidade Federal de Minas Gerais (CM-UFGM), and from AngloGold Ashanti, who provided insights and expertise that greatly assisted this research; Fundação para a Ciência and Tecnologia (FCT) for financial aid; and Vanessa Soares for laboratory support and reuse tests using nanofibers.

**Conflicts of Interest:** The authors declare no conflict of interest.

## References

1. Lowry, G.V.; Shaw, S.; Kim, C.S.; Rytuba, J.J.; Brown, G.E. Macroscopic and microscopic observations of particle-facilitated mercury transport from New Idria and Sulphur Bank mercury mine tailings. *Environ. Sci. Technol.* **2004**, *38*, 5101–5111. [[CrossRef](#)] [[PubMed](#)]
2. Ma, J.; Lei, M.; Weng, L.; Li, Y.; Chen, Y.; Islam, M.S.; Zhao, J.; Chen, T. Fractions and colloidal distribution of arsenic associated with iron oxide minerals in lead-zinc mine-contaminated soils: Comparison of tailings and smelter pollution. *Chemosphere* **2019**, *227*, 614–623. [[CrossRef](#)] [[PubMed](#)]
3. Moreno, F.; Valente, T.M.F.; Gomes, P.; Fonseca, R.; Costa, M.R.; Costa, A. Partitioning of Potentially Toxic Elements among Two Colloidal Fractions and Relevance for Their Mobility in Different Water Types. In Proceedings of the 16th International Symposium on Water-Rock Interaction (WRI-16) and 13th International Symposium on Applied Isotope Geochemistry (1st IAGC International Conference), Tomsk, Russia, 21–26 July 2019. [[CrossRef](#)]
4. Jackson, L.M.; Parbhakar-Fox, A. Mineralogical and geochemical characterization of the Old Tailings Dam. Australia: Evaluating the effectiveness of a water cover for long-term AMD control. *Appl. Geochem.* **2016**, *68*, 64–78. [[CrossRef](#)]
5. Martínez, J.; Hidalgo, M.C.; Rey, J.; Garrido, J.; Kohfahl, C.; Benavente, J.; Rojas, D. A multidisciplinary characterization of a tailings pond in the Linares-La Carolina mining district. Spain. *J. Geochem. Explor.* **2016**, *162*, 62–71. [[CrossRef](#)]
6. Araujo, F.S.; Taborda-Llano, I.; Nunes, E.B.; Santos, R.M. Recycling and reuse of mine tailings: A review of advancements and their implications. *Geosciences* **2022**, *12*, 319. [[CrossRef](#)]
7. Cacciuttolo, C.; Cano, D. Environmental Impact Assessment of Mine Tailings Spill Considering Metallurgical Processes of Gold and Copper Mining: Case Studies in the Andean Countries of Chile and Peru. *Water* **2022**, *14*, 3057. [[CrossRef](#)]
8. Lemos, M.; Valente, T.; Reis, P.M.; Fonseca, R.; Pantaleão, J.P.; Guabiroba, F.; Filho, J.G.; Magalhães, M.; Afonseca, B.; Silva, A.R.; et al. Geochemistry and mineralogy of auriferous tailings deposits and their potential for reuse in Nova Lima Region. Brazil. *Sci. Rep.* **2023**, *13*, 4339. [[CrossRef](#)]
9. Acheampong, M.A.; Adiyiah, J.; Ansa, E.D.O. Physico-chemical characteristics of a gold mining tailings dam wastewater. *J. Environ. Sci. Eng.* **2013**, *A2*, 469–475.
10. Economopoulos, A.P. *Assessment of Sources of Air, Water and Soil Pollution: A Guide to Rapid Source Inventory Techniques and Their Use in Formulating Environmental Control Strategies*; World Health Organization: Geneva, Switzerland, 1993; 230p.
11. Puls, R.W.; Powell, R.M. Transport of inorganic colloids through natural aquifer material: Implications for contaminant transport. *Environ. Sci. Technol.* **1992**, *26*, 614–621.
12. Modi, S.; Yadav, V.K.; Gacem, A.; Ali, I.H.; Dave, D.; Khan, S.H.; Yadav, K.K.; Rather, S.; Ahn, Y.; Son, C.T.; et al. Recent and emerging trends in remediation of methylene blue dye from wastewater by using zinc oxide nanoparticles. *Water* **2022**, *14*, 1749. [[CrossRef](#)]
13. Maharajh, D.; Grewar, T.; Neale, J.; van Rooyen, M. Mine Water: A Resource for the Circular Economy in South African Mining Communities. In Proceedings of the Mine Water Solutions, Vancouver, Canada, 12–16 June 2018; pp. 349–362.
14. Stevanović, Z.; Obradović, L.; Marković, R.; Jonović, R.; Avramović, L.; Bugarin, M.; Stevanović, J. Mine waste water management in the Bor municipality in order to protect the Bor River water. In *Water Water-Treatment Technologies and Recent Analytical Developments*; Einschlag, F.S.G., Ed.; InTech: Rijeka, Croatia, 2013; pp. 41–62.
15. Wastewater Characterization Study. TRC Environmental Corporation. Available online: [https://www.ibwc.gov/Files/Characterization\\_Study\\_March\\_2015.pdf](https://www.ibwc.gov/Files/Characterization_Study_March_2015.pdf) (accessed on 6 June 2023).
16. Leroy, M.N.L.; Richard, M.J.; Mouhamed, A.N.; Sifeu, T.K.; Yvan, A.S.R.; Said, R. Physicochemical characterization of mining waste from the Betare-Oya gold area (East Cameroon) and an adsorption test by Sabga smectite (North-West Cameroon). *Scientifica* **2020**, *2020*, 6293819. [[CrossRef](#)]
17. Etteieb, S.; Magdouli, S.; Zolfaghari, M.; Brar, S. Monitoring and analysis of selenium as an emerging contaminant in mining industry: A critical review. *Sci. Total Environ.* **2020**, *698*, 134339. [[CrossRef](#)] [[PubMed](#)]
18. Dippong, T.; Mihali, C.; Hoaghia, M.A.; Cical, E.; Cosma, A. Chemical modeling of groundwater quality in the aquifer of Seini town–Somes Plain, Northwestern Romania. *Ecotoxicol. Environ. Saf.* **2019**, *168*, 88–101. [[CrossRef](#)]
19. Rostami, A.A.; Isazadeh, M.; Shahabi, M.; Nozari, H. Evaluation of geostatistical techniques and their hybrid in modelling of groundwater quality index in the Marand Plain in Iran. *Environ. Sci. Pollut. Res.* **2019**, *26*, 34993–35009. [[CrossRef](#)] [[PubMed](#)]
20. Rashid, A.; Ayub, M.; Ullah, Z.; Ali, A.; Sardar, T.; Iqbal, J.; Gao, X.; Bundschuh, J.; Li, C.; Khattak, S.A.; et al. Groundwater Quality, Health Risk Assessment, and Source Distribution of Heavy Metals Contamination around Chromite Mines: Application of GIS, Sustainable Groundwater Management, Geostatistics, PCAMLR, and PMF Receptor Model. *Int. J. Environ. Res. Public Health* **2023**, *20*, 2113. [[CrossRef](#)]
21. Yadav, K.K.; Gupta, N.; Kumar, V.; Choudhary, P.; Khan, S.A. GIS-based evaluation of groundwater geochemistry and statistical determination of the fate of contaminants in shallow aquifers from different functional areas of Agra city, India: Levels and spatial distributions. *RSC Adv.* **2018**, *8*, 15876–15889. [[CrossRef](#)] [[PubMed](#)]
22. Nas, B. Geostatistical Approach to Assessment of Spatial Distribution of Groundwater Quality. *Pol. J. Environ. Stud.* **2019**, *18*, 1073–1082.
23. Sonia; Ghosh, T.; Gacem, A.; Alsufyani, T.; Alam, M.M.; Yadav, K.K.; Amanullah, M.; Cabral-Pinto, M.M.S. Geospatial Evaluation of Cropping Pattern and Cropping Intensity Using Multi Temporal Harmonized Product of Sentinel-2 Dataset on Google Earth Engine. *Appl. Sci.* **2022**, *12*, 12583. [[CrossRef](#)]

24. Naranjo-Fernández, N.; Guardiola-Albert, C.; Montero-González, E. Applying 3D Geostatistical Simulation to Improve the Groundwater Management Modelling of Sedimentary Aquifers: The Case of Doñana (Southwest Spain). *Water* **2019**, *11*, 39. [[CrossRef](#)]
25. França, S.C.; Andrade, L.S.; Loayza, P.E.; Trampus, B.C. Water in Mining—Challenges for Reuse. In Proceedings of the 13th International Mine Water Association Congress—Mine Water & Circular Economy, Lappeenranta, Finland, 25–30 June 2017.
26. Semenkov, I.; Sharapova, A.; Lednev, S.; Yudina, N.; Karpachevskiy, A.; Klink, G.; Koroleva, T. Geochemical Partitioning of Heavy Metals and Metalloids in the Ecosystems of Abandoned Mine Sites: A Case Study within the Moscow Brown Coal Basin. *Water* **2022**, *14*, 113. [[CrossRef](#)]
27. Domingues, A.F.; Boson, P.H.G.; Alípaz, S. *Water Resource Management and the Mining Industry*; Instituto Brasileiro de Mineração: Brasília, Brazil, 2013; 336p.
28. Yadav, K.K.; Gupta, N.; Kumar, V.; Sharma, S.; Arya, S. Water quality assessment of Pahuj River using water quality index at Unnao Balaji, MP, India. *Int. J. Sci. Basic Appl. Res.* **2015**, *19*, 241–250.
29. Dang, H.T.; Tran, H.D.; Tran, N.T.; Tran, A.H.; Sasakawa, M. Potential Reuse of Coal Mine Wastewater: A Case Study in Quang Ninh, Vietnam. In Proceedings of the 37th WEDC International Conference, Hanoi, Vietnam, 15–19 September 2014.
30. Huertas, E.; Salgot, M.; Hollender, J.; Weber, S.; Dott, W.; Khan, S.; Schafer, A.; Messalem, R.; Bis, B.; Aharoni, A.; et al. Key objectives for water reuse concepts. *Desalination* **2008**, *218*, 120–131. [[CrossRef](#)]
31. Meng, S.; Wen, S.; Han, G.; Wang, X.; Feng, Q. Wastewater treatment in mineral processing of non-ferrous metal resources: A review. *Water* **2022**, *14*, 726. [[CrossRef](#)]
32. Maurya, P.K.; Ali, S.A.; Zaidi, S.K.; Wasi, S.; Tabrez, S.; Malav, L.C.; Dittthakit, P.; Com, C.T.; Cabral-Pinto, M.M.S.; Yadav, K.K. Assessment of groundwater geochemistry for drinking and irrigation suitability in Jaunpur district of Uttar Pradesh using GIS-based statistical inference. *Environ. Sci. Pollut. Res.* **2023**, *30*, 29407–29431. [[CrossRef](#)]
33. Zhang, C.; Wen, L.; Wang, Y.; Liu, C.; Zhou, Y.; Lei, G. Can constructed wetlands be wildlife refuges? A review of their potential biodiversity conservation value. *Sustainability* **2020**, *12*, 1442. [[CrossRef](#)]
34. Rajpar, M.N.; Ahmad, S.; Zakaria, M.; Ahmad, A.; Guo, X.; Nabi, G.; Wanghe, K. Artificial wetlands as alternative habitat for a wide range of waterbird species. *Ecol. Indic.* **2022**, *138*, 108855. [[CrossRef](#)]
35. Mohapatra, D.P.; Kirpalani, D.M. Process effluents and mine tailings: Sources, effects and management and role of nanotechnology. *Nanotechnol. Environ. Eng.* **2017**, *2*, 1. [[CrossRef](#)]
36. Araya, N.; Ramírez, Y.; Kraslawski, A.; Cisternas, L.A. Feasibility of re-processing mine tailings to obtain critical raw materials using real options analysis. *J. Environ. Manag.* **2021**, *284*, 112060. [[CrossRef](#)]
37. Atlagić, S.G.; Tankosić, L.; Pržulj, S.; Mirošljević, D. Recent Patents in Reuse of Metal Mining Tailings and Emerging Potential in Nanotechnology Applications. *Recent Pat. Nanotechnol.* **2021**, *15*, 256–269. [[CrossRef](#)] [[PubMed](#)]
38. Moreira, V.R.; Lebron, Y.A.R.; Gontijo, D.; Amaral, M.C.S. Membrane distillation and dispersive solvent extraction in a closed-loop process for water, sulfuric acid and copper recycling from gold mining wastewater. *Chem. Eng. J.* **2022**, *435*, 133874. [[CrossRef](#)]
39. Sharma, G.K.; Jena, R.K.; Ray, P.; Yadav, K.K.; Moharana, P.C.; Cabral-Pinto, M.M.; Bordoloi, G. Evaluating the geochemistry of groundwater contamination with iron and manganese and probabilistic human health risk assessment in endemic areas of the world's largest River Island, India. *Environ. Toxicol. Pharmacol.* **2021**, *87*, 103690. [[CrossRef](#)] [[PubMed](#)]
40. DuChanois, R.M.; Cooper, N.J.; Lee, B.; Patel, S.K.; Mazurowski, L.; Graedel, T.E.; Elimelech, M. Prospects of metal recovery from wastewater and brine. *Nat. Water* **2023**, *1*, 37–46. [[CrossRef](#)]
41. Nakhjiri, A.T.; Sanaeepur, H.; Amooghin, A.E.; Shirazi, M.M.A. Recovery of precious metals from industrial wastewater towards resource recovery and environmental sustainability: A critical review. *Desalination* **2022**, *527*, 115510. [[CrossRef](#)]
42. Ahmed, M.; Mavukkandy, M.O.; Giwa, A.; Elektorowicz, M.; Katsou, E.; Khelifi, O.; Naddeo, V.; Hasan, S.W. Recent developments in hazardous pollutants removal from wastewater and water reuse within a circular economy. *NPJ Clean Water* **2022**, *5*, 12. [[CrossRef](#)]
43. Soares, V.A.A.P. Recuperação de Metais Estratégicos au (iii), ag (i), pt (iv) e pd (ii) de Barragens de Rejeito e Lixo Eletrônico Com o Uso de Nanotecnologia e Urucum Visando Tecnologias Sustentáveis: Uma Proposta Translacional. Ph.D. Thesis, Universidade Federal de Minas Gerais, Belo Horizonte, Brazil, 2022.
44. Kumar, M.; Nandi, M.; Pakshirajan, K. Recent advances in heavy metal recovery from wastewater by biogenic sulfide precipitation. *J. Environ. Manag.* **2021**, *278*, 111555. [[CrossRef](#)]
45. Wang, F.; Lu, X.; Li, X.Y. Selective removals of heavy metals (Pb<sup>2+</sup>, Cu<sup>2+</sup>, and Cd<sup>2+</sup>) from wastewater by gelation with alginate for effective metal recovery. *J. Hazard. Mater.* **2016**, *308*, 75–83. [[CrossRef](#)] [[PubMed](#)]
46. Reis, B.G. Toward High Temperature and Low pH Gold Mining Effluent Reclamation by Different Membrane Separation Processes. Ph.D. Thesis, Universidade Federal de Minas Gerais, Belo Horizonte, Brazil, 2018.
47. Urkiaga, A.; Fuentes, L.D.; Bis, B.; Chiru, E.; Balasz, B.; Hernández, F. Development of analysis tools for social, economic and ecological effects of water reuse. *Desalination* **2008**, *218*, 81–91. [[CrossRef](#)]
48. Lemos, M.; Valente, T.; Reis, P.M.; Fonseca, R.; Delbem, I.; Ventura, J.; Magalhães, M. Mineralogical and geochemical characterization of gold mining tailings and their potential to generate acid mine drainage (Minas Gerais, Brazil). *Minerals* **2020**, *11*, 39. [[CrossRef](#)]



49. Goldfarb, R.J.; Groves, D.I.; Gardoll, S. Orogenic gold and geologic time: A global synthesis. *Ore Geol. Rev.* **2001**, *18*, 1–75. [[CrossRef](#)]
50. Lobato, L.M.; Ribeiro-Rodrigues, L.C.; Vieira, F.W.R. Brazil's premier gold province. Part II: Geology and genesis of gold deposits in the Archean Rio das Velhas greenstone belt, Quadrilátero Ferrífero. *Miner. Depos.* **2001**, *36*, 249–277. [[CrossRef](#)]
51. AGA. AngloGold Ashanti AngloGold Ashanti Recommendations. 2021; (Unpublished).
52. Eaton, A.D.; Clesceri, L.S.; Rice, E.W.; Greenberg, A.E.; Franson, M.A.H. *Standard Method for Examination of Water and Wastewater*, 21st ed.; American Public Health Association: Washington, DC, USA, 2005.
53. Pereira, M.S. Avaliação dos Produtos de Oxidação e Ocorrência do Efeito Preg-Robbing da Oxidação sob Pressão em Autoclave de Bancada e Industrial Para o Minério Sulfetado da Mina I de Córrego do Sítio, Minas Gerais. Master's Thesis, Universidade Federal de Minas Gerais, Belo Horizonte, Brazil, 2020.
54. Magalhães, M.F. Utilização de Simulação de Elementos Discretos (DEM) Para Avaliação de Parâmetros da Teoria da Amostragem. Ph.D. Thesis, Universidade de São Paulo, São Paulo, Brazil, 2022.
55. Lemos, M.G.; Valente, T.M.F.; Reis, A.P.M.; Fonsceca, R.; Dumont, J.M.; Ferreira, G.M.M.; Delbem, I.D. Geoenvironmental study of gold mining tailings in a circular economy context: Santa Barbara, Minas Gerais, Brazil. *Mine Water Environ.* **2021**, *40*, 257–269. [[CrossRef](#)]
56. Moura, W. Especificação de Cianeto para Redução do Consumo no Circuito de Lixiviação de Calcinado da Usina do Queiróz. Master Thesis, Universidade Federal de Minas Gerais, Belo Horizonte, Brazil, 2005.
57. Instituto Brasileiro de Geografia e Estatística—IBGE. Available online: <https://www.ibge.gov.br/023> (accessed on 28 June 2023).
58. Gomes, F.P.S.S. Impactos dos Processos de Drenagem Ácida na Qualidade Ambiental e Acumulação Potencial de Metais Estratégicos em Barragens Localizadas na Faixa Piritosa Ibérica. Ph.D. Thesis, Universidade do Minho, Braga, Portugal, 2021.
59. Acosta, J.A.; Cano, A.F.; Arocena, J.M.; Debela, F.; Martínez-Martínez, S. Distribution of metals in soil particle size fractions and its implication to risk assessment of playgrounds in Murcia City (Spain). *Geoderma* **2009**, *149*, 101–109. [[CrossRef](#)]
60. Wilson, R.; Toro, N.; Naranjo, O.; Emery, X.; Navarra, A. Integration of geostatistical modeling into discrete event simulation for development of tailings dam retreatment applications. *Miner. Eng.* **2021**, *164*, 106814. [[CrossRef](#)]
61. Dinpashoh, Y.; Jahanbakhsh-Asl, S.; Rasouli, A.A.; Foroughi, M.; Singh, V.P. Impact of climate change on potential evapotranspiration (case study: West and NW of Iran). *Theor. Appl. Climatol.* **2019**, *136*, 185–201. [[CrossRef](#)]
62. Biazar, S.M.; Dinpashoh, Y.; Singh, V.P. Sensitivity analysis of the reference crop evapotranspiration in a humid region. *Environ. Sci. Pollut. Res.* **2019**, *26*, 32517–32544. [[CrossRef](#)] [[PubMed](#)]
63. Gomes, P.; Valente, T.; Cordeiro, M.; Moreno, F. Hydrochemistry of Pit Lakes in the Portuguese Sector of the Iberian Pyrite Belt. In Proceedings of the 16th International Symposium on Water-Rock Interaction (WRI-16) and 13th International Symposium on Applied Isotope Geochemistry (1st IAGC International Conference), Tomsk, Russia, 21–26 July 2019; E3S Web of Conferences, EDP Sciences. Volume 98, p. 09007. [[CrossRef](#)]
64. Conselho Nacional do Meio Ambiente (Brasil). Resolução, n° 357, de 17 de Março de 2005. In Proceedings of the Dispõe Sobre a Classificação dos Corpos de Água e Diretrizes Ambientais Para o Seu Enquadramento, Bem Como Estabelece as Condições e Padrões de Lançamento de Efluentes, e dá Outras Providências, Diário Oficial da União, Brasília, Brazil, 17 March 2005.
65. Junqueira, P.A.; Lobato, L.M.; Ladeira, E.A.; Simões, E.J.M. Structural control and hydrothermal alteration at the BIF-hosted Raposos lode-gold deposit, Quadrilátero Ferrífero, Brazil. *Ore Geol. Rev.* **2007**, *32*, 629–650. [[CrossRef](#)]
66. Valente, T.M.F. Modelos de Caracterização de Impacte Ambiental para Escombrelas Reactivas: Equilíbrio e Evolução de Resíduos de Actividade Extractiva. Ph.D. Thesis, Universidade do Minho, Braga, Portugal, 2004.
67. Deschamps, E.; Ciminelli, V.S.; Lange, F.T.; Matschullat, J.; Raue, B.; Schmidt, H. Soil and sediment geochemistry of the iron quadrangle, Brazil the case of arsenic. *J. Soils Sediments* **2002**, *2*, 216–222. [[CrossRef](#)]
68. Krauskopf, K.B. Separation of manganese from iron in sedimentary processes. *Geochim. Cosmochim. Acta* **1957**, *12*, 61–84. [[CrossRef](#)]
69. Rahighi, R.; Hosseini-Hosseiniabad, S.M.; Zeraati, A.S.; Suwaileh, W.; Norouzi, A.; Panahi, M.; Gholipour, S.; Karaman, C.; Akhavan, O.; Kholari, M.A.R.; et al. Two-dimensional materials in enhancement of membrane-based lithium recovery from metallic-ions-rich wastewaters: A review. *Desalination* **2022**, *543*, 116096. [[CrossRef](#)]
70. Millan, R.D.S.; Galery, R.; Costa, L.M.; Windmoeller, C.C.; Soares, V.A.A.P.; Diniz, A.G.N.; Amador, V.S. Processo para tratamento de efluentes e recuperação de metais nobres com uso de sementes de *Bixa orellana*. Linnaeus. Patent BR1020210263202, 23 December 2021.

**Disclaimer/Publisher's Note:** The statements, opinions and data contained in all publications are solely those of the individual author(s) and contributor(s) and not of MDPI and/or the editor(s). MDPI and/or the editor(s) disclaim responsibility for any injury to people or property resulting from any ideas, methods, instructions or products referred to in the content.